

1 The Problem

We consider a feedforward neural network with a single hidden layer and activation function σ . It receives an input $x \in \mathbb{R}^n$ and produces a scalar output $\hat{y} \in \mathbb{R}$. The hidden layer has K units. The weights for the first and second layer are $W_1 \in \mathbb{R}^{K \times n}$ and $W_2 \in \mathbb{R}^{1 \times K}$, respectively, and the corresponding biases are $b_1 \in \mathbb{R}^K$ and $b_2 \in \mathbb{R}$.

$$\hat{y} = W_2 \sigma(W_1 x + b_1) + b_2. \quad (1)$$

Our data x are sampled from a mixture of two translation-invariant distributions in some family $\{p_\xi\}_\xi$ parameterized by a correlation length-scale ξ . That is, we sample $x \sim p_{\xi_1}$ with probability $\frac{1}{2}$ and $x \sim p_{\xi_2}$ otherwise. If x is sampled from p_{ξ_1} , then $y(x) = 1$; otherwise, $y(x) = 0$. We can train using either mean-squared error or cross-entropy loss, though we primarily consider the former.

Alessandro’s paper primarily considers the case where $W_2 = \frac{1}{K} \mathbf{1}^\top$ (take the mean of the hidden activations) is fixed and $\sigma(h) = \text{erf}(\frac{h}{\sqrt{2}})$. I have also tried $\sigma = \text{sigmoid}, \text{ReLU}$. For the former, the results are qualitatively identical, while for the latter we get localization if $\xi_1 > \xi_2$ and short-range oscillations otherwise. For $\sigma = \text{ReLU}$, one can further remove the bias terms b_1 and b_2 (though not for sigmoid).

We consider two types of datasets: the nonlinear Gaussian process (NLGP) and the single pulse (SP). We explain them in more detail later. They differ primarily in that the former has continuous support on \mathbb{R}^n , while the latter has discrete support on a subset of $\{0, 1\}^n$. The former also has a gain parameter that controls the degree of localization, while the latter does not.

We’ll present the results in reverse order, since it makes more sense logically. We start by attempting to analyze the ReLU model directly. This will force us to assume Gaussian data, which captures only half of what we’d like to describe. We will discuss some ideas about how to extend this to the non-Gaussian case, and perhaps also the SP dataset.

To address these analytical roadblocks, we’ll explore using a gated deep linear network (GDLN) to model the ReLU network. This will require some assumptions about the gating structure, which we test empirically. However, we’re not really sure how to properly set up the “neural race” and map the winner onto the ReLU case. We consider a few approaches, though we are not sure which is correct. We’ll conclude with some questions, concerns, and ideas, with specific focus on the discrete Fourier transform, uncertainty principle, and characteristic functions.

2 ReLU Analysis

Let’s start by trying to analyze the gradient flow for a ReLU network. We won’t be able to solve it exactly, but we can get some intuition. We will have to assume the data are Gaussian to say something interesting after just a few steps. Of course, this is the case we are less interested in, since it’s the non-Gaussian data that shows localization.

Let w_i be the i -th row in W_1 . We make predictions with

$$\hat{y}(x) = \frac{1}{K} \sum_{k \in [K]} \text{ReLU}(\langle w_k, x \rangle). \quad (2)$$

We use MSE loss,

$$\mathcal{L} = \frac{1}{2} \mathbb{E}_{X,Y} \left[(\hat{y}(X) - Y)^2 \right]. \quad (3)$$

The corresponding gradient flow for w_1 is given by

$$\tau \frac{d}{dt} w_1 = - \mathbb{E}_{X,Y} \left[\left(\frac{1}{K} \sum_{k \in [K]} \text{ReLU}(\langle w_k, X \rangle) - Y \right) \frac{\partial}{\partial w_1} [\text{ReLU}(\langle w_1, X \rangle)] \right] \quad (4)$$

$$= \frac{1}{2} \mathbb{E}_{X, \langle w_1, X \rangle > 0 | Y=1} [X] - \frac{1}{K} \sum_{k \in [K]} \mathbb{E}_{X,Y, \langle w_1, X \rangle > 0, \langle w_k, X \rangle > 0} [\langle w_k, X \rangle X] \quad (5)$$

Gaussian Data

To compute these conditional expectations, we will have to assume the data are Gaussian. We begin by computing the first conditional expectation. Define the random variable $S = \langle w_1, X \rangle$.

$$\mathbb{E}_{X, S > 0 | Y=1} [X] = \mathbb{E}_{S > 0 | Y=1} [\mathbb{E}_{X|S,Y=1} [X]]. \quad (6)$$

Let us consider X sampled from p_{ξ_1} (i.e. with label $Y = 1$) and write

$$X = AX + Sv, \quad (7)$$

where

$$v = \frac{1}{w_1^\top \Sigma_1 w_1} \Sigma_1 w_1, \quad (8)$$

$$A = I_n - v w_1^\top. \quad (9)$$

Equation (7) clearly holds. Our specific selection of v and A guarantees that AX and S have zero covariance. *Since X is Gaussian, this implies they are independent.* So, $X | S \sim \mathcal{N}(Sv, A\Sigma_1 A^\top)$. Note that $\mathbb{E}_{S|S>0,Y=1} [S] = \left(\frac{2}{\pi} w_1^\top \Sigma_1 w_1\right)^{\frac{1}{2}}$. Plugging this into equation (6),

$$\mathbb{E}_{X, S > 0 | Y=1} [X] = \mathbb{E}_{S > 0 | Y=1} [Sv] \quad (10)$$

$$= \mathbb{E}_{S|S>0,Y=1} [Sv] \mathbb{P}(S > 0 | Y = 1) \quad (11)$$

$$= \frac{1}{\sqrt{2\pi}} (w_1^\top \Sigma_1 w_1)^{-\frac{1}{2}} \Sigma_1 w_1. \quad (12)$$

Now, let us evaluate the second conditional expectation. First, we consider the case $k = 1$. Then, we only have one positivity constraint. We use S again, just as before. Let us also only consider X with label $Y = 1$. Both labels appear in the ODE for this term, but the result has the same form.

$$\mathbb{E}_{X, S > 0 | Y=1} [SX] = \mathbb{E}_{S > 0 | Y=1} [S \mathbb{E}_{X|S,Y=1} [X]] \mathbb{P}(S > 0 | Y = 1) = \mathbb{E}_{S|S>0,Y=1} [S^2] v \mathbb{P}(S > 0 | Y = 1). \quad (13)$$

By symmetry of S about 0, $\mathbb{E}_{S|S>0,Y=1} [S^2] = \mathbb{E}_{S|Y=1} [S^2] = w_1^\top \Sigma_1 w_1$. (This step does not require Gaussianity!) So,

$$\mathbb{E}_{X, \langle w_1, X \rangle > 0 | Y=1} [\langle w_1, X \rangle X] = \frac{1}{2} w_1^\top \Sigma_1 w_1 \left(\frac{1}{w_1^\top \Sigma_1 w_1} \Sigma_1 w_1 \right) = \frac{1}{2} \Sigma_1 w_1. \quad (14)$$

Now, let us consider $k > 1$. We will need to consider both positivity constraints. This is going to get really messy! I will skip the analysis here and just present the final result. (See an earlier version of this document for all the steps.)

We'll need to define some more variables to make things a bit more compact.

$$\rho_{ij} = w_i^\top \Sigma w_j \quad \text{for } i, j = 1, k \quad \text{and} \quad \gamma = \frac{\rho_{1k}}{\sqrt{\rho_{11}\rho_{kk}}}. \quad (15)$$

In toto,

$$\mathbb{E}_{X, \langle w_1, X \rangle > 0, \langle w_k, X \rangle > 0 | Y=1} [\langle w_k, X \rangle X] \quad (16)$$

$$= \left[\frac{1}{2\pi(1-\gamma^2)} \left(\frac{\rho_{kk}}{\rho_{11}} \cos^{-1}(-\gamma) - \gamma^2 \sin^{-1}(\gamma) \right) + \frac{\frac{1}{\gamma\rho_{11}} - \frac{1}{\sqrt{\rho_{11}\rho_{kk}}}}{2\pi\sqrt{1-\gamma^2}} \right] \Sigma_1 w_1 \quad (17)$$

$$+ \left[-\frac{\gamma}{2\pi(1-\gamma^2)} \sqrt{\frac{\rho_{11}}{\rho_{kk}}} \left(\frac{\rho_{kk}}{\rho_{11}} \cos^{-1}(\gamma) - \sin^{-1}(\gamma) \right) + \frac{\frac{1}{\gamma\rho_{kk}} - \frac{1}{\sqrt{\rho_{11}\rho_{kk}}}}{2\pi\sqrt{1-\gamma^2}} \right] \Sigma_1 w_k$$

$$= \left[\frac{\gamma^2 - \frac{\rho_{kk}}{\rho_{11}}}{2\pi(1-\gamma^2)} \cos^{-1}(\gamma) + \frac{2\frac{\rho_{kk}}{\rho_{11}} - \gamma^2}{4(1-\gamma^2)} + \frac{\frac{1}{\gamma\rho_{11}} - \frac{1}{\sqrt{\rho_{11}\rho_{kk}}}}{2\pi\sqrt{1-\gamma^2}} \right] \Sigma_1 w_1 \quad (18)$$

$$+ [\text{? some mess ?}] \Sigma_1 w_k$$

A single neuron Let's consider what happens if we have just one hidden neuron, i.e. $K = 1$. Then, the above analysis simplifies greatly. The gradient flow becomes

$$\tau \frac{d}{dt} w_1 = \frac{1}{2} \mathbb{E}_{X, \langle w_1, X \rangle > 0 | Y=1} [X] - \mathbb{E}_{X, Y, \langle w_1, X \rangle > 0} [\langle w_1, X \rangle X] \quad (19)$$

$$= -\frac{1}{4} \left(\Sigma_0 + \left(1 - \sqrt{\frac{2}{\pi}} (w_1^\top \Sigma_1 w_1)^{-\frac{1}{2}} \right) \Sigma_1 \right) w_1. \quad (20)$$

Recall that both Σ_0 and Σ_1 are circulant, so they diagonalize in the discrete Fourier transform basis. (Actually, since they are real, symmetric matrices, they diagonalize in the discrete sine/cosine transform basis.) Let us analyze w_1 in this basis by defining $u_1 = F^\top w_1$, where F is the discrete sine/cosine transform matrix. Let Λ_0 and Λ_1 be the diagonal matrices of eigenvalues for Σ_0 and Σ_1 , respectively. Then,

$$\tau \frac{d}{dt} u_1 = -\frac{1}{4} \left(\Lambda_0 + \left(1 - \sqrt{\frac{2}{\pi}} (u_1^\top \Lambda_1 u_1)^{-\frac{1}{2}} \right) \Lambda_1 \right) u_1. \quad (21)$$

Figure 1 establishes the validity of equation (21) for Gaussian data. (Note the empirical and theoretical receptive fields are slightly different because the former uses minibatches while the latter uses the full dataset, and also because of a possible slight issue with learning rates. If both of these are extended to infinity, they align almost perfectly, but I wanted to show the evolution as well.)

Finding u_1 We can't solve this ODE exactly, but we can try to find its steady state. Write $\|u_1\|_{\Lambda_1} = \sqrt{u_1^\top \Lambda_1 u_1}$. Then, setting equation (21) to 0 yields

$$(\Lambda_0 + \Lambda_1)u_1 = \sqrt{\frac{2}{\pi}} \frac{1}{\|u_1\|_{\Lambda_1}} \Lambda_1 u_1. \quad (22)$$

We can look at this entrywise:

$$(\lambda_0^{(k)} + \lambda_1^{(k)})u_1^{(k)} = \sqrt{\frac{2}{\pi}} \frac{\lambda_1^{(k)}}{\|u_1\|_{\Lambda_1}} u_1^{(k)}. \quad (23)$$

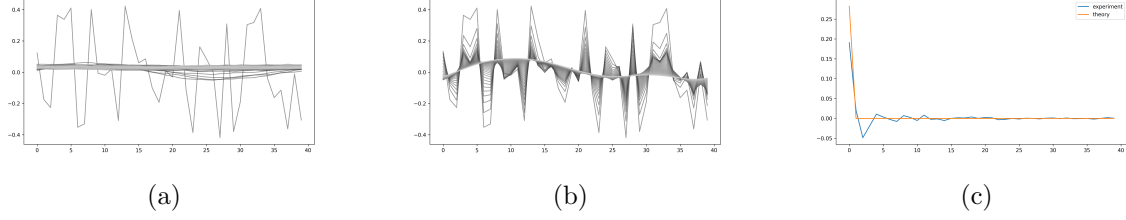


Figure 1: Time-evolution of empirical (a) and theoretical (b) receptive fields for a single neuron with Gaussian data, along with (c) the final empirical vs. theoretical receptive fields in frequency space. Task settings: $\xi_1 = 2, \xi_2 = 1, g = 0.01, n = 40$. Training settings: learning rate of 0.01, batch size of 10,000, and 2,000 training steps with evaluations every 20. Model settings: $K = 1$ with w_1 initialized from an Xavier normal with scale 1.

If $u_1^{(k)} \neq 0$, then

$$\frac{\lambda_0^{(k)}}{\lambda_1^{(k)}} + 1 = \sqrt{\frac{2}{\pi}} \frac{1}{\|u_1\|_{\Lambda_1}}. \quad (24)$$

So, in order for $u_1^{(k)}$ to be nonzero, we need the above equation to hold. Note the right side is fixed for all k . So we need $\frac{\lambda_0^{(k)}}{\lambda_1^{(k)}}$ to be constant for all k such that $u_1^{(k)}$ is nonzero.

Recall we defined our eigenvectors to be the real and imaginary parts of the columns of the discrete Fourier transform, with the exception of the first and last eigenvectors. So, eigenvalues will come in pairs, with the exception of the first and last eigenvalues. Empirically, we observe that these pairs are all distinct. So, only one or two of the eigenvectors will ever be nonzero. If it is one, we will have

$$\frac{\lambda_0^{(k)}}{\lambda_1^{(k)}} + 1 = \sqrt{\frac{2}{\pi}} \frac{1}{(u_1^{(k)})^2 \lambda_1^{(k)}} \iff (u_1^{(k)})^2 = \sqrt{\frac{2}{\pi}} \frac{1}{\lambda_0^{(k)} + \lambda_1^{(k)}}. \quad (25)$$

If it is two, we will see a superposition of the real and imaginary parts of the corresponding discrete Fourier transform column.

$$\frac{\lambda_0^{(k_1)}}{\lambda_1^{(k_1)}} + 1 = \frac{\lambda_0^{(k_2)}}{\lambda_1^{(k_2)}} + 1 = \sqrt{\frac{2}{\pi}} \frac{1}{(u_1^{(k_1)})^2 \lambda_1^{(k_1)} + (u_1^{(k_2)})^2 \lambda_1^{(k_2)}} \quad (26)$$

$$\sqrt{\frac{2}{\pi}} = \left(\frac{\lambda_0^{(k_1)}}{\lambda_1^{(k_1)}} + 1 \right) \left((u_1^{(k_1)})^2 \lambda_1^{(k_1)} + (u_1^{(k_2)})^2 \lambda_1^{(k_2)} \right) \quad (27)$$

$$= \lambda_0^{(k_1)} (u_1^{(k_1)})^2 + \frac{\lambda_0^{(k_1)} \lambda_1^{(k_2)}}{\lambda_1^{(k_1)}} (u_1^{(k_2)})^2 + (u_1^{(k_1)})^2 \lambda_1^{(k_1)} + (u_1^{(k_2)})^2 \lambda_1^{(k_2)} \quad (28)$$

$$= [\lambda_0^{(k_1)} + \lambda_1^{(k_1)}] (u_1^{(k_1)})^2 + \left[\frac{\lambda_0^{(k_1)}}{\lambda_1^{(k_1)}} + 1 \right] \lambda_1^{(k_2)} (u_1^{(k_2)})^2. \quad (29)$$

Similarly,

$$\sqrt{\frac{2}{\pi}} = \left(\frac{\lambda_0^{(k_2)}}{\lambda_1^{(k_2)}} + 1 \right) \left((u_1^{(k_1)})^2 \lambda_1^{(k_1)} + (u_1^{(k_2)})^2 \lambda_1^{(k_2)} \right) \quad (30)$$

$$= \left[\frac{\lambda_0^{(k_2)}}{\lambda_1^{(k_2)}} + 1 \right] \lambda_1^{(k_1)} (u_1^{(k_1)})^2 + [\lambda_0^{(k_2)} + \lambda_1^{(k_2)}] (u_1^{(k_2)})^2. \quad (31)$$

We could solve for $u_1^{(k_1)}$ and $u_1^{(k_2)}$ in terms of $\lambda_0^{(k_1)}, \lambda_1^{(k_1)}, \lambda_0^{(k_2)}, \lambda_1^{(k_2)}$. But what's the point right now?

We still do not know which eigenvalues will be nonzero. Empirically, in the *very long limit*, it's only the first eigenvalue that is nonzero. This corresponds to a flat receptive field. Interestingly, for the data shown above, $k = 1$ has the smallest ratio $\frac{\lambda_0^{(k)}}{\lambda_1^{(k)}}$ and the smallest inverse sum $\frac{1}{\lambda_0^{(k)} + \lambda_1^{(k)}}$. I think this means its update is affected least by changes in $\|u_1\|_{\Lambda_1}$. I am not sure if this will generalize.

Conclusion Recall that we need to assume the data are Gaussian to conclude that AX and S are independent. This is necessary to compute the conditional expectations. One would hope that the general form remains the same for non-Gaussian data, but we cannot say anything precise. One might assume that the case that the change in the distribution of the eigenvalues for Σ_1 and Σ_0 alone might account for this difference. However, recall that the eigenvalues are derived from the covariance matrix, which is just a second-order statistic. So, a Gaussian with the same covariance matrix would have the same eigenvalues. However, Alessandro showed that if you train on Gaussian with covariance matching the non-Gaussian case, you do not get localization. So, there is something other than just modifying Λ_1 and Λ_0 that changes the dynamics in equation (21) in the non-Gaussian case.

It is surprising that $w_1(t)$ pops out of the input-output term. This *does not happen in the gated linear network*, and this might be a key difference. What does this say about gating early during training?

Fourier transforms Above, we just introduced the discrete Fourier transform matrix without explaining what it looks like. Now, we'll quickly explain what it is and how we can simplify it when we have a real symmetric circulant matrix.

In a nutshell, circulant matrices diagonalize in the discrete Fourier basis because they act as convolutions on vectors. This is clear from their definition:

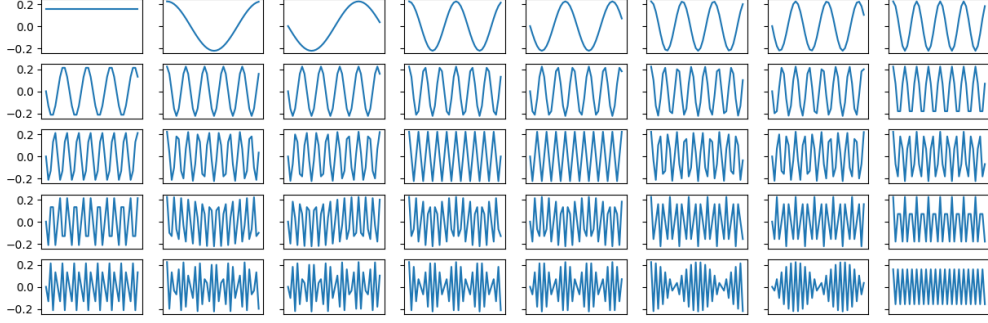
$$\Sigma = \begin{bmatrix} c_0 & c_{n-1} & \cdots & c_2 & c_1 \\ c_1 & c_0 & c_{n-1} & & c_2 \\ \vdots & c_1 & c_0 & \ddots & \vdots \\ c_{n-2} & & \ddots & \ddots & c_{n-1} \\ c_{n-1} & c_{n-2} & \cdots & c_1 & c_0 \end{bmatrix}. \quad (32)$$

It is easiest to understand the discrete Fourier transform matrix P by seeing how its columns are constructed:

$$F_{:,j} = v_j \equiv \frac{1}{\sqrt{n}} \begin{bmatrix} 1 \\ \omega^j \\ \omega^{2j} \\ \vdots \\ \omega^{(n-1)j} \end{bmatrix} = \frac{1}{\sqrt{n}} \begin{bmatrix} 1 \\ \cos(\frac{2\pi}{n}j) \\ \cos(\frac{2\pi}{n}2j) \\ \vdots \\ \cos(\frac{2\pi}{n}(n-1)j) \end{bmatrix} - \frac{i}{\sqrt{n}} \begin{bmatrix} 0 \\ \sin(\frac{2\pi}{n}j) \\ \sin(\frac{2\pi}{n}2j) \\ \vdots \\ \sin(\frac{2\pi}{n}(n-1)j) \end{bmatrix}, \quad (33)$$

where $\omega = e^{-\frac{2\pi i}{n}}$. So, each column is a sinusoid of an increasing frequency. These columns are unit vectors and orthogonal to each other. So, when we multiply a vector by F , we compute its coefficient w.r.t. to this basis. This is analogous to computing the Fourier transform of a signal.

When our circulant matrix is real and symmetric ($c_i = c_{n-i} \forall 1 \leq i < n$), we know from the spectral decomposition that we could diagonalize it using real eigenvectors. Specifically, we can use the real and

Figure 2: Discrete sine/cosine transform matrix F for $n = 40$.

imaginary parts of the columns of P :

$$\Sigma(\operatorname{Re} v_j) = \operatorname{Re}(\Sigma v_j) = \operatorname{Re}(\lambda_j v_j) = \lambda_j(\operatorname{Re} v_j), \quad (34)$$

since the eigenvalues are real. We can do the same for the imaginary parts. Then, we just need to select the real and imaginary parts of the columns of F to get a real orthogonal matrix. Notice an immediate redundancy in the real parts:

$$\operatorname{Re} v_j = \frac{1}{\sqrt{n}} \begin{bmatrix} 1 \\ \cos(\frac{2\pi}{n}j) \\ \cos(\frac{2\pi}{n}2j) \\ \vdots \\ \cos(\frac{2\pi}{n}(n-1)j) \end{bmatrix} = \frac{1}{\sqrt{n}} \begin{bmatrix} 1 \\ \cos(\frac{2\pi}{n}(n-1)j) \\ \cos(\frac{2\pi}{n}(n-2)j) \\ \vdots \\ \cos(\frac{2\pi}{n}j) \end{bmatrix} = \operatorname{Re} v_{n-j}. \quad (35)$$

So, we only need to consider the real parts of first $\frac{n}{2}$ columns of F . The same can be said for the imaginary parts, though we ignore the first column since it is all zeros, and take the $\frac{n}{2} + 1$ -th real column in its place. If we sort the columns by frequency, we get the sinusoids shown in figure 2.

Non-Gaussian Data

We needed Gaussianity to say that AX and S were independent. Our construction of v and A was chosen to make AX and S have zero covariance. For general data, this does not imply independence. So, we will have to do something else to compute the conditional expectations.

What do we know about X ? First, it is symmetric about 0, and it is translation invariant. As $g \rightarrow \infty$, $X_i(Z) \xrightarrow{d} \operatorname{sign}(Z_i)$. Deriving the pmf of X in this limit amounts to solving the “orthant problem” for multivariate normals. For inputs of dimension larger than 4, this is an open research problem. So, I don’t think we’ll have much luck here. For what it’s worth, we don’t need full information about the distribution, just the conditional expectations. But I struggle to see how we could compute this if we cannot even compute the pmf.

Basis initialization What if we initialize the weights to be the basis vectors for \mathbb{R}^n ? (This is the same as the “small bump” gate we show below.) I am going to break the law and cite that result here without showing any work. For $X \triangleq \operatorname{erf}(gZ)$,

$$\mathbb{E}_{X, \langle X, e_i \rangle > 0 | Y=1} [\langle X, e_i \rangle] \quad (36)$$

Uncertainty Principle

Sometimes, the receptive fields we get *really* look like (the real part of) Gabors. This really seems to be the case when we have multiple hidden neurons and high gain. We can show that the receptive fields continuously deform from long-range oscillations to localized bumps as we increase the gain. If the receptive fields actually are Gabors, this could be explained by variations in the exponential decay and sinusoidal frequency terms in the Gabor’s definition. *A hypothesis I would like to test is that in both the Gaussian and non-Gaussian cases, the receptive fields are 1-d Gabor wavelets, differing only in the decay and frequency terms.*

This would be a very strong result, and I am not sure how to prove it. One possible strategy is to connect this to the uncertainty principle. The idea would be to show that the receptive fields’ uncertainties in position and frequency decrease during training to the theoretical minimum of $\frac{1}{2}$. Showing this minimum is attained seems quite challenging, but perhaps we can at least show that the uncertainty decreases monotonically.

There are three immediate difficulties here. First, the signals can be complex-valued, while here we only wish to consider real-valued signals. (What is a complex-valued receptive field anyway?) So, we would need to figure out what the uncertainty principle looks like for real continuous signals, and hopefully then also discrete ones. Secondly, the uncertainty principle was established for the Fourier transform, not the discrete Fourier transform. That is, the inputs are continuous, not discrete. Finally, are receptive fields seem to be periodic, while the uncertainty principle is for non-periodic signals. I am not sure if it is actually true that our receptive fields are periodic, but it seems to me that an uncertainty-minimizing signal on the 1-d torus would look very different from that on the real line. I will try to address these three concerns in the following paragraphs.

The uncertainty principle First, I introduce the classical uncertainty principle for complex-valued, continuous signals on the real line.

3 Have You Tried Making It Linear?

Gating lets us decompose the ReLU post-activation in terms of the pre-activation’s sign and magnitude.

$$\text{ReLU}(\langle w_1(t), x \rangle) = g(t, x) \langle w_1(t), x \rangle \quad \text{where} \quad g(t, x) = \mathbb{1}(\langle w_1(t), x \rangle \geq 0). \quad (37)$$

We generally assume that g does not vary during learning, even though w_1 may. Later on, we’ll try to analyze what happens when this does not hold.

To assess the validity of this assumption, we need to see how much $g(x)$, as defined above, changes during learning. Additionally, post-hoc, we can usually pick a somewhat sensible gating structure that mimics a specific run’s behavior. But we’d like to be able to determine this gating upfront. We explore all this in the following subsections.

3.1 Sign Flipping

We will model the ReLU network as in equation (37), focusing on how g varies with time for each hidden neuron. We will look at the metric

$$p(t) = \mathbb{P}_x(g(t, x) = g(t + \delta t, x)) \quad \text{for all } t. \quad (38)$$

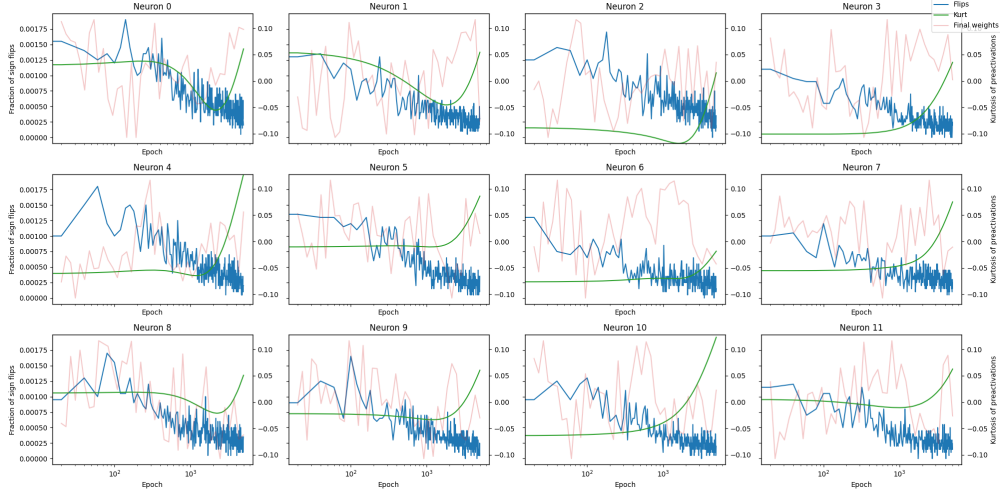


Figure 3: Sign flipping in the NLGP dataset. Blue shows $p(t)$ across t . Green shows excess kurtosis of preactivations to a single neuron. Red shows the final receptive fields for the corresponding neuron. Task settings: $\xi_1 = 2, \xi_2 = 1, g = 0.01, n = 40$. Training settings: learning rate of 0.01, batch size of 10,000, and 5,000 training steps with evaluations every 20. Model settings: $K = 12$ with weights initialized from an Xavier normal with scale 1.

Note that g is invariant to the scale of w_1 . We observe in the experiments above that w_1 appears to grow uniformly in size during much of its training, appearing as if it’s just being scaled up towards its final value. If this isn’t true in position space, it seems more likely to be true in frequency space, though it only seems to really hold in the long-range oscillation case. This is probably not a very good assumption during the early stage of training, but it seems more plausible once they have stabilized a bit. There is, importantly, a phase where the receptive field goes from Gaussian to non-Gaussian, but the shape it assumes at the end of training emerges quite quickly. This suggests that $g(x)$ may be relatively constant during learning, at least after the initial phase. If this is so, then it would be reasonable to try using a standard GDLN to model the ReLU network.

This is precisely what we check in figure 3. We see that at any given time, gates, on average, flip sign for a very small fraction of the data, and this happens less as training progresses. However, the fact that there is still some sign flipping means we cannot—with confidence—naively apply a GDLN to model the ReLU network. We will try this next, but it’s not obvious what the gates should be a priori, which lead us to questions about how to interpret the neural race.

3.2 Predicting Loca(liza)tion

TODO: can we predict where localization will occur a priori?

4 Let's Consider a Single Layer with Linear Activation...

Our GDLN model is defined as follows:

$$\hat{y}(x) = \frac{1}{K} \left(\sum_{k \in [K]} g_k(x) w_k^\top \right) x, \quad (39)$$

where g_k are (node) gates. Again, $w_k \in \mathbb{R}^n$ are the rows of the first-layer weight matrix $W_1 \in \mathbb{R}^{K \times n}$. That is,

$$W_1 = \begin{pmatrix} w_1^\top \\ \vdots \\ w_K^\top \end{pmatrix} \quad (40)$$

Recalling the GDLN paper, the gradient flow for w_1 is given by

$$\tau \frac{d}{dt} w_1 = \frac{1}{K} \left[\Sigma^{yx}(p_1) - \sum_{k \in [K]} \Sigma^{xx}(p_1, p_k) w_k \right], \quad (41)$$

where

$$\Sigma^{yx}(p_i) = \mathbb{E}_{g,X,Y} [g_i Y X] \quad (42)$$

$$\Sigma^{xx}(p_i, p_j) = \mathbb{E}_{g,X,Y} [g_i g_j X X^\top]. \quad (43)$$

All rows w_k of W_1 have gradient flows of this form. Let us analyze them all simultaneously. To do so, let us relabel $b_i = \Sigma^{yx}(p_i)$ and $A_{ij} = \Sigma^{xx}(p_i, p_j)$. Note that A_{ij} is symmetric and $A_{ij} = A_{ji}$. Then, we can write the gradient flow for all weights as

$$K\tau \frac{d}{dt} \underbrace{\begin{bmatrix} w_1 \\ \vdots \\ w_K \end{bmatrix}}_{w \in \mathbb{R}^{Kn}} = \underbrace{\begin{bmatrix} b_1 \\ \vdots \\ b_K \end{bmatrix}}_{b \in \mathbb{R}^{Kn}} - \underbrace{\begin{bmatrix} A_{11} & \cdots & A_{1K} \\ \vdots & \ddots & \vdots \\ A_{K1} & \cdots & A_{KK} \end{bmatrix}}_{A \in \mathbb{R}^{Kn \times Kn}} \underbrace{\begin{bmatrix} w_1 \\ \vdots \\ w_K \end{bmatrix}}_{w \in \mathbb{R}^{Kn}}. \quad (44)$$

Observe that w is the vectorized form of our $K \times n$ first-layer weight matrix. Note also that A is a symmetric real matrix, so we can diagonalize it as $A = P\Lambda P^\top$, where the columns of P are the eigenvectors of A and the diagonal entries of Λ are the corresponding (nonnegative) eigenvalues. To see this more clearly, let us write

$$\tilde{g}(x) = \begin{bmatrix} g_1(x) \\ \vdots \\ g_K(x) \end{bmatrix}. \quad (45)$$

Then,

$$A = \langle (\tilde{g} \otimes X)(\tilde{g} \otimes X)^\top \rangle_{g,X}, \quad (46)$$

which is clearly a symmetric matrix.

We can reparameterize in terms of $u = P^\top w$ and $c = P^\top b$.

$$K\tau \frac{d}{dt}u = -\Lambda u + c \implies u(t) = \Lambda^{-1}e^{-\frac{t}{K\tau}\Lambda+C}\mathbf{1} + \Lambda^{-1}c, \quad (47)$$

where C is a constant diagonal matrix that defines the initial condition. So,

$$w(t) = P\Lambda^{-1}e^{-\frac{t}{K\tau}\Lambda+C}\mathbf{1} + P\Lambda^{-1}c \quad (48)$$

$$= A^{-1}Pe^{-\frac{t}{K\tau}\Lambda+C}\mathbf{1} + A^{-1}b. \quad (49)$$

Exclusive Gates Let us assume that the gates are exclusive, that is, only one gate is active at a time. Then, $\Sigma^{xx}(p, q) = 0$ for $p \neq q$, which makes A block diagonal. We can write the gradient flow for w_1 as

$$K\tau \frac{d}{dt}w_1 = -A_{11}w_1 + b_1. \quad (50)$$

Note that $A_{11} = \Sigma^{xx}(p_1, p_1)$ is always symmetric (and real). So, we can diagonalize it to solve the ODE. If we do this, we get

$$w_1(\infty) = (\Sigma^{xx}(p_1, p_1))^{-1} \left(Pe^{-\frac{t}{K\tau}\Lambda+C}\mathbf{1} + \Sigma^{yx}(p_1)^\top \right), \quad (51)$$

where C is some constant diagonal matrix that defines the initial condition. As with above, this is the population solution to OLS, $(\mathbb{E}_{X,Y}[XX^\top])^{-1}\mathbb{E}_{X,Y}[YX]$. So, each weight matrix converges to the OLS solution on the subset of the data determined by its gate.

4.1 Winning Gating Structure

Can we read off the winning gating structure from the equations above? This is where we are unsure of how exactly to interpret the “neural race.” Is the idea that the gating structure that learns fastest in the GDLN is the one the ReLU network ends up implementing? Or, is the idea to do some meta-optimization over gating structures to minimize the limiting loss of the corresponding GDLN, and propose that this is what ReLU somehow “knows” to use? Are both perspectives insightful or meaningful?

We would answer the former by looking at the induced eigenvalues of A . The “race winner” would be that which yields the smallest eigenvalues. We would answer the latter by looking at the limiting loss of the GDLN. The winner would be that which yields the smallest loss in the limit. Both of these seem like complicated, though certainly empirically investigable, problems (though, the space of gates to search over is combinatorially large, if not infinite!). We empirically analyze a few gating structures below.

4.1.1 Do We Care About Early Dynamics?

We wish to see which gating structures yield solutions with the smallest eigenvalues, since they will decay the slowest. **However, we have many eigenvalues, so which ones do we look at?**

For small t , but sufficiently large to see separation among different eigenvalues, can we predict the leading structure?

TODO: look into eigenvalues for some gating structures! (Pick random, zero, and localized, for example.)

4.1.2 Or Limiting Behavior?

If none of the eigenvalues are zero, then $w(\infty) = A^{-1}b$. If we write

$$\tilde{x} = \begin{bmatrix} g_1(x)x \\ \vdots \\ g_K(x)x \end{bmatrix} \in \mathbb{R}^{Kn}, \quad (52)$$

then $A = \mathbb{E}_{g,X,Y} [\tilde{X}\tilde{X}^\top]$ and $b = \mathbb{E}_{g,X,Y} [Y\tilde{X}]$. Then, it is clear that this is the population solution to the OLS problem of regressing Y on \tilde{X} , averaging across the distributions of the data *subject to* the gating architecture.

In this context, one might ask, which gating structure minimizes the MSE loss? The loss is (note we use $\langle \rangle$ notation for brevity):

$$\mathcal{L}_\infty = \left\langle \left(\tilde{X}'^\top (\langle \tilde{X}\tilde{X}^\top \rangle_{g,X,Y})^{-1} \langle Y\tilde{X} \rangle_{g,X,Y} - Y' \right)^2 \right\rangle_{g',X',Y'} \quad (53)$$

$$= \left\langle (\tilde{X}'^\top (\langle \tilde{X}\tilde{X}^\top \rangle_{g,X,Y})^{-1} \langle Y\tilde{X} \rangle_{g,X,Y})^2 - 2(Y'\tilde{X}'^\top (\langle \tilde{X}\tilde{X}^\top \rangle_{g,X,Y})^{-1} \langle Y\tilde{X} \rangle_{g,X,Y}) + (Y')^2 \right\rangle_{g',X',Y'} \quad (54)$$

$$= \frac{1}{2} - \langle Y\tilde{X}^\top \rangle_{g,X,Y} (\langle \tilde{X}\tilde{X}^\top \rangle_{g,X,Y})^{-1} \langle Y\tilde{X} \rangle_{g,X,Y} \quad (55)$$

$$= \frac{1}{2} - \frac{1}{2} \langle \tilde{X} \rangle_{g,X|Y=1}^\top (\langle \tilde{X}\tilde{X}^\top \rangle_{g,X|Y=1} + \langle \tilde{X}\tilde{X}^\top \rangle_{g,X|Y=0})^{-1} \langle \tilde{X} \rangle_{g,X|Y=1}. \quad (56)$$

The “meta-optimization” question is: For fixed p_{ξ_1} and p_{ξ_2} , how do we choose the gates g_k to minimize equation (56)?

It may be useful to write this in terms of Kronecker products. Let

$$\tilde{g}(x) = \begin{bmatrix} g_1(x) \\ \vdots \\ g_K(x) \end{bmatrix} \in \{0,1\}^K. \quad (57)$$

Then, minimizing equation (56) is equivalent to maximizing

$$\mathcal{L}_\infty^*(\tilde{g}) = \langle \tilde{g} \otimes X \rangle_{g,X|Y=1}^\top (\langle (\tilde{g} \otimes X)(\tilde{g} \otimes X)^\top \rangle_{g,X|Y=1} + \langle (\tilde{g} \otimes X)(\tilde{g} \otimes X)^\top \rangle_{g,X|Y=0})^{-1} \langle \tilde{g} \otimes X \rangle_{g,X|Y=1} \quad (58)$$

over $\tilde{g} : \text{supp}(p_{\xi_1}) \cup \text{supp}(p_{\xi_2}) \rightarrow \{0,1\}^K$.

4.2 Structure in Limiting Behavior

The limiting solution in equation (51) assumes, of course, that the gates are fixed throughout training. As we observe in figure 3, the gates stabilize relatively early on. Our ReLU analysis was able to fully explain the behavior of a single neuron if we train with Gaussian data. With the GDLN, if we know what the gate, $g(x)$, stabilizes to, then we can use the limiting solution to fully characterize the final receptive fields for both Gaussian *and* non-Gaussian data.

Let us consider a gate of the form $g(x) = \mathbb{1}(\langle e_i, x \rangle > 0)$. This gate is turned on only when the i -th coordinate of x is positive. This is a simple case of a localized bump (and much easier to analyze). We’ll show that it explains the localization behavior we’ve observed in the converged weights of the ReLU network.

Input-output covariance The interesting structure is in the input-output covariance. Let's compute it.

$$\Sigma^{yx}(p_i) = \mathbb{E}_{g,X,Y} [g_i Y X] \quad (59)$$

$$= \mathbb{E}_{X, \langle e_i, X \rangle > 0 | Y=1} [X] \mathbb{P}(Y=1) \quad (60)$$

$$= \mathbb{E}_{Z_i > 0} \left[\mathbb{E}_{Z | Z_i, Y=1} \left[\frac{\text{erf}(gZ)}{\mathcal{Z}(g)} \right] \right] \mathbb{P}(Y=1). \quad (61)$$

In the final step, we use the fact that $X_i > 0 \iff Z_i > 0$. This is not true if we take an inner product with something other than e_i —*this is a big part of what makes the nonlinear case so hard to analyze*. Here, $\mathcal{Z}(g)$ is the normalization constant that ensures the variance of each coordinate is 1 for all $g > 0$, which here represents the gain. (Sorry about overloading notation here! In the GDLN work, g is the gate, but in Alessandro's work it is the gain. I didn't want to switch existing notation too much, and I think it's clear from context which one we mean.)

Let us evaluate the inner expectation. We will suppress the conditioning on $Y=1$ for brevity. Note that for $j \neq i$, $Z_j | Z_i \sim \mathcal{N}(rZ_i, 1 - r^2)$, where r is the covariance between Z_i and Z_j , which is equal to $e^{-(i-j)^2/\xi_1^2}$. Thus,

$$\mathbb{E}_{Z | Z_i, Y=1} [\text{erf}(gZ_j)] = \int_{\mathbb{R}} \text{erf}(gz_j) \frac{1}{\sqrt{2\pi}\sqrt{1-r^2}} \exp\left(-\frac{(z_j - rz_i)^2}{2(1-r^2)}\right) dz_j \quad (62)$$

$$= \text{erf}\left(\frac{gr}{\sqrt{1+2g^2(1-r^2)}} z_i\right). \quad (63)$$

Now, we can compute the outer expectation.

$$\mathbb{E}_{Z_i > 0} [\mathbb{E}_{Z | Z_i, Y=1} [\text{erf}(gZ_j)]] = \int_0^\infty \frac{1}{\sqrt{2\pi}} \exp\left(-\frac{z_i^2}{2}\right) \text{erf}\left(\frac{gr}{\sqrt{1+2g^2(1-r^2)}} z_i\right) dz_i \quad (64)$$

$$= \frac{2}{\sqrt{\pi}} \tan^{-1}\left(\frac{\sqrt{2}gr}{\sqrt{1+2g^2(1-r^2)}}\right) \quad (65)$$

$$= \frac{2}{\sqrt{\pi}} \tan^{-1}\left(\frac{r}{\sqrt{\frac{1}{2g^2} + (1-r^2)}}\right). \quad (66)$$

In summary,

$$\Sigma^{yx}(p_i)_j = \frac{1}{\sqrt{\pi}\mathcal{Z}(g)} \tan^{-1}\left(\frac{r}{\sqrt{\frac{1}{2g^2} + (1-r^2)}}\right). \quad (67)$$

Visualizing this in figure 4, we see that it produces a localized bump centered at i . This is cool! But what does the input-input covariance term do? Well, for this gate, it basically computes a difference between adjacent points of $\Sigma^{yx}(p_i)$.

TODO: finish!

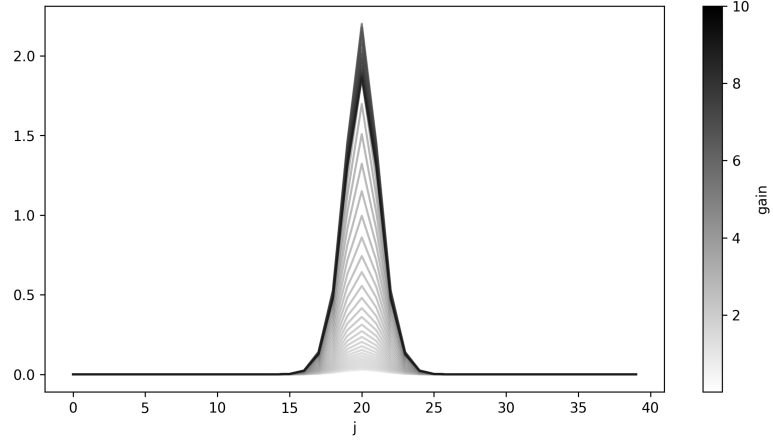


Figure 4: Entries j of input-output covariance $\Sigma^{yx}(p_i)$ for $i = 20$ for varying g .

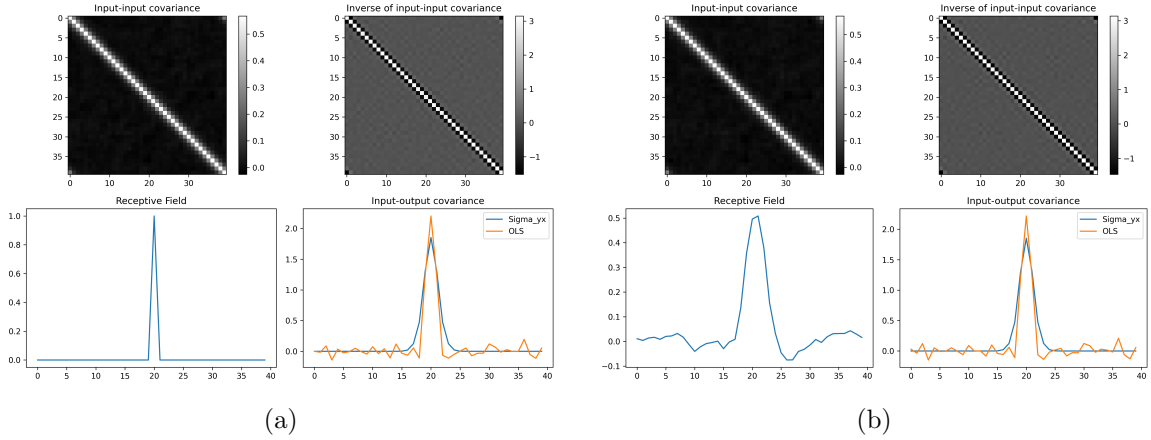


Figure 5: Input-input covariance, its inverse, the receptive field used to define the gate, and its effect on shaping $\Sigma^{yx}(p_i)$ to determine the OLS solution for (a) small-bump and (b) Mexican-hat-like receptive fields.

5 Stability of Localization

5.1 Linear Pathway

5.2 Student-Teacher

6 Theory-driven Experiments

6.1 General Case

6.2 Single Gate

6.3 Redundant Gates